

## Edge and bulk effects in Terahertz photoconductivity of an antidot superlattice

B. G. L. Jäger,<sup>1</sup> S. Wimmer,<sup>1</sup> A. Lorke,<sup>1,2</sup> J. P. Kotthaus,<sup>1</sup> W. Wegscheider,<sup>3,\*</sup> and M. Bichler<sup>3</sup>  
<sup>1</sup>*Sektion Physik and Center for NanoScience, Ludwig-Maximilians-Universität München, Geschwister-Scholl-Platz 1, D-80539 München, Germany*  
<sup>2</sup>*Laboratorium für Festkörperphysik, Gerhard-Mercator-Universität, Lotharstrasse 17, D-47048 Duisburg, Germany*  
<sup>3</sup>*Walter Schottky Institut, TU München, Am Coulombwall D-85748 Garching, Germany*  
 (Received 19 May 2000; published 9 January 2001)

We investigate the terahertz (THz) response of a square antidot superlattice by means of photoconductivity measurements using a Fourier-transform-spectrometer. We detect, spectrally resolved, the cyclotron resonance and the fundamental magnetoplasmon mode of the periodic superlattice. In the dissipative transport regime both resonances are observed in the photoresponse. In the adiabatic transport regime, at integer filling factor  $\nu=2$ , only the cyclotron resonance is observed. From this we infer that different mechanisms contribute to converting the absorption of THz radiation into photoconductivity in the cyclotron and in the magnetoplasmon resonances. In the dissipative transport regime, heating of the electrons via resonant absorption of the THz radiation in the two-dimensional bulk is the main mechanism of photoconductivity in both resonances. In the case of the cyclotron resonance, and especially in the adiabatic transport regime, we find an additional contribution to photoconductivity which we interpret as being caused by THz-absorption-induced backscattering of edge states. The characteristic decay length of the magnetoplasmon at the sample edges is about an order of magnitude larger than the typical width of the edge states in the quantum Hall effect. The magnetoplasmon is therefore not able to induce such backscattering of edge states. Thus in the adiabatic transport regime, i.e., when only the edge states contribute to electric conduction, magnetoplasmon excitation does not induce a photoconductive signal.

DOI: 10.1103/PhysRevB.63.045315

PACS number(s): 73.20.Mf, 73.43.-f, 73.50.Pz

### I. INTRODUCTION

The magnetotransport properties of a two-dimensional electron gas (2DEG) in high magnetic fields are successfully described in the edge channel or Landauer-Büttiker picture.<sup>1-4</sup> According to this model the spatial current distribution in a 2DEG in high magnetic fields is strongly influenced by the filling factor of the 2DEG. At the edges of a Hall bar the Landau levels (LL's) of the unbounded 2DEG are bent upward in energy due to the confining potential. The intersections of these upwardly bent Landau levels with the Fermi energy form the so-called edge states.<sup>5-7</sup> Electrons in edge states at opposite edges of the Hall bar flow in opposite directions. At integer filling factors the Fermi energy lies in the regime of localized states between two Landau levels of the 2D bulk, and a sufficiently small electric current is carried by the edge states only. In thermal equilibrium all edge states at the same sample edge have the same chemical potential. Scattering between edge states of the same sample edge (inter-LL scattering) is likely to occur after a distance that is called the equilibration length  $l_{eq}$ . However, this kind of scattering event does not lead to a nonzero magnetoresistance  $\rho_{xx}$  along the current direction as it cannot reverse an electron's direction of motion. Over distances up to the equilibration length a nonequilibrium population between edge states (of the same edge) can be maintained. The transport regime in which no equilibration between edge states (of the same edge) occurs is called the adiabatic regime. At non-integer filling factors the Fermi energy lies within the topmost partially filled Landau level. This topmost (further also referred to as  $N$ th) Landau level can form a bulk conduction channel that allows backscattering of electrons, which

leads to a nonzero longitudinal magnetoresistance  $\rho_{xx}$ .<sup>8,9</sup> The  $N$ th channel is almost perfectly decoupled from the lower  $N-1$  edge states.<sup>8</sup> This means that the edge states propagate unaffected by the bulk channel just as they would do for integer filling factors.

Here we study the photoconductivity of nanostructured 2DEG's caused by intraband absorption in the quantum Hall regime. Intraband photoconductivity<sup>10</sup> of 2DEG's has been successfully described by Neppel *et al.*<sup>11</sup> using a bolometric model, which was originally employed to explain the mechanism of photoconductivity caused by intersubband resonance in 2DEG's. Later the same model was also applied to cyclotron-resonance-induced photoconductivity in the quantum Hall regime<sup>12</sup> and to photoconductivity of systems with reduced dimensionality.<sup>13</sup> In cyclotron resonance, the absorption of radiation excites single electrons from the  $(N-1)$ st (bulk) LL below the Fermi energy to the  $N$ th LL above the Fermi energy. Within a bolometric model the excited electrons thermalize via electron-electron interactions and a new quasiequilibrium corresponding to a higher electron temperature is established. As the longitudinal resistance  $\rho_{xx}$  depends on temperature, the increased electron temperature results in a change of the longitudinal resistance,  $\Delta\rho_{xx}$ , which is measured in a photoconductivity experiment.

In more recent photoconductivity experiments, an enhanced cyclotron resonance amplitude in the adiabatic transport regime close to a current injecting contact<sup>14</sup> was observed. The longitudinal resistance in the adiabatic regime at low temperatures and bias currents under illumination by a far-infrared laser was observed to show a sharp maximum<sup>15</sup> at the cyclotron resonance. The authors concluded that the cyclotron resonance absorption process induces a nonequi-

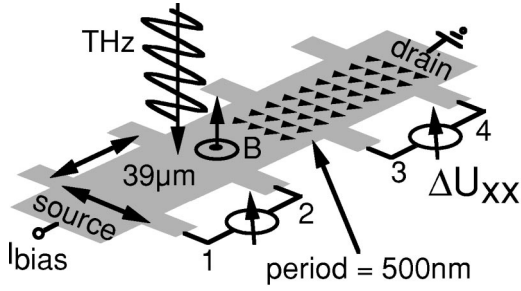


FIG. 1. Sample layout and setup for photoconductivity measurements.

librium population of edge states. They infer that this also leads to interedge scattering (i.e., to scattering events that are able to reverse the electrons' direction of motion) and thus to an increase in longitudinal resistance. This increase in resistance can be observed directly in photoconductivity<sup>14</sup> and in magnetotransport.<sup>15</sup>

We investigate the photoconductivity properties of an antidot superlattice which allows us to excite the cyclotron resonance and the fundamental magnetoplasmon mode by illumination with THz radiation. We find that at noninteger filling factors mainly resonant electron heating contributes to photoconductivity in both absorption processes. Under adiabatic transport conditions at a filling factor of  $\nu=2$ , on the contrary, only the cyclotron resonance (CR) is observed. Here, in addition, the CR amplitude has a different dependence on the applied bias current than the magnetoplasmon and cyclotron resonance amplitudes in the dissipative transport regime. This indicates that the photoresponse in the adiabatic transport regime is generated by a process different from electron heating, which is mainly responsible for the photosignal in the dissipative regime.

## II. SAMPLE DETAILS AND EXPERIMENTAL TECHNIQUE

The sample investigated here is a square antidot superlattice with a period of 500 nm, fully covering the distance of 39  $\mu\text{m}$  between adjacent voltage probes on a 39  $\mu\text{m}$  wide Hall bar (Fig. 1).

The antidot superlattice is prepared on a GaAs/AlGaAs heterostructure with a mobility (at  $T=4.2$  K) of  $\mu = 15.3$   $\text{cm}^2/\text{Vs}$  and an electron density  $n_s = 3.45 \times 10^{15}$   $\text{m}^{-2}$  in the unpatterned 2DEG. The 2DEG is a distance of 37 nm from the sample surface. The antidots are written by  $e$ -beam lithography and transferred into the 2DEG by shallow ( $\approx 6$  nm) wet etching. In the patterned region the density (obtained by Hall measurements) is smaller by about 7% compared to the unpatterned 2DEG. The antidots have a triangular shape (width 300 nm, height 200 nm).<sup>16</sup> However, this is not essential for the results presented here.

We study the photoresponse, in particular the change in resistance  $\Delta R_{xx} = \Delta U_{xx}/I$ , in response to the THz illumination, by measuring the photoinduced voltage  $\Delta U_{xx}$  between two voltage probes in four-point geometry as shown in Fig. 1. We apply dc bias currents  $I$  of up to 10  $\mu\text{A}$  between source and drain contacts. The bath temperature during the

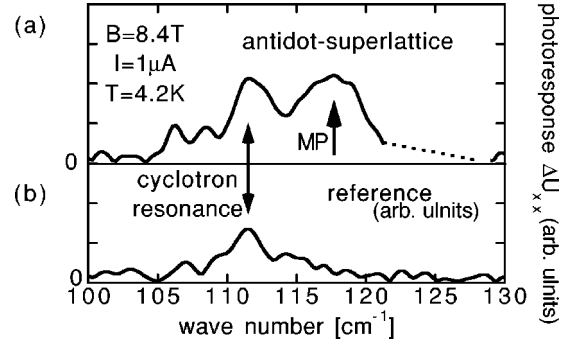


FIG. 2. Photoresponse  $\Delta U_{xx}$  at a bias current of  $I=1$   $\mu\text{A}$  and a magnetic field of  $B=8.4$  T for (a) the antidot superlattice and (b) the unpatterned reference section. In the dashed part of curve (a) an artifact has been removed.

measurements is 4.2 K, and magnetic fields of up to 12 T are applied perpendicular to the plane of the 2DEG.

We use a broadband mercury lamp to irradiate our samples. The light source is modulated by a Fourier-transform spectrometer to spectrally analyze the measured photoresponse  $\Delta U_{xx}$ . In the spectral range of interest to us, between 0 and 200  $\text{cm}^{-1}$  (0–6 THz), the Hg lamp has an integrated intensity of a few microwatts.

## III. EXPERIMENTAL RESULTS

In Fig. 2(a) typical data in the dissipative regime at a magnetic field of 8.4 T ( $\nu \approx 1.6$ ) and a bias current of 1  $\mu\text{A}$  applied from the source to the drain contact are shown. As can be seen there, we detect the cyclotron resonance and a magnetoplasmon (MP) resonance. The photoresponse  $\Delta U_{xx}$  was recorded between contacts 3 and 4. Figure 2(b) shows a spectrum taken at the reference section on the same Hall bar (contacts 1 and 2). There, only the cyclotron resonance is resolved.

We record the photoresponse spectra for a series of magnetic fields between 0 and 12 T and fit the spectral resonance position of the magnetoplasmon as a function of the applied magnetic field by<sup>17,20</sup>  $\omega^2 = \omega_0^2 + \omega_c^2$  to extrapolate the zero-magnetic-field plasmon frequency  $\omega_0$ . This  $\omega_0$  is compared to the calculated frequency  $\omega_p$  of a plasmon in a two-dimensional electron gas with a two-dimensional modulation of the charge density with periods  $a_x$  and  $a_y$  along the  $x$  and  $y$  directions, respectively. We determine  $\omega_p$  from sample-specific parameters via the formula<sup>18,19</sup>

$$\begin{aligned} \omega_p^2 &= \frac{N_s e^2}{2m^* \epsilon_{eff} \epsilon_0} \sqrt{\left(n_x \frac{2\pi}{a_x}\right)^2 + \left(n_y \frac{2\pi}{a_y}\right)^2} \\ &= \frac{N_s e^2}{2m^* \epsilon_{eff}(k) \epsilon_0} k. \end{aligned} \quad (1)$$

Here,  $n_x$  and  $n_y$  are integers,  $N_s$  is the 2D electron density,  $m^*$  the effective mass,  $k$  the wave vector as defined by the above formula, and  $\epsilon_{eff}$  the effective dielectric constant. In the present case  $a_x = a_y = a = 500$  nm. For  $\epsilon_{eff}$  we use<sup>17</sup>  $\epsilon_{eff}(k) = \epsilon_{\text{GaAs}} / [1 + (\epsilon - 1) / (\epsilon + 1) e^{-2kd}]$ , where the dis-

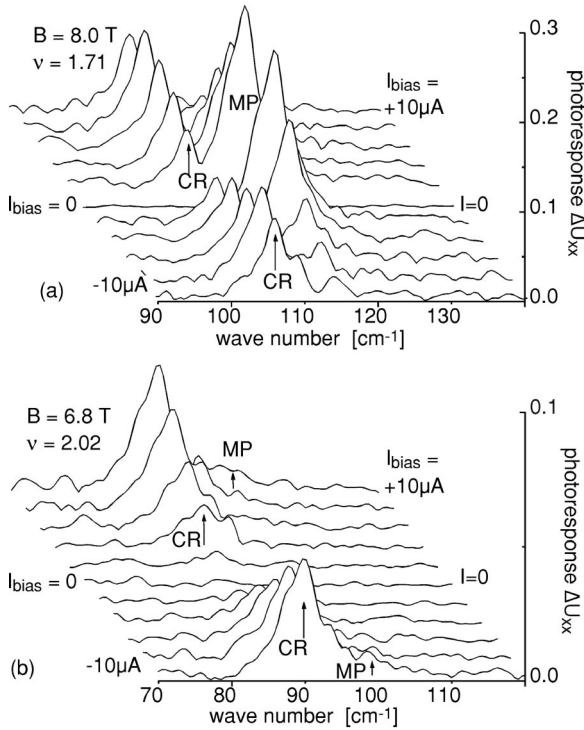


FIG. 3. Photoconductivity spectra at a magnetic field (filling factor) of (a)  $B = 8$  T ( $\nu = 1.7$ ) and (b)  $B = 6.8$  T ( $\nu = 2$ ) for different bias currents ranging from  $I = -10 \mu\text{A}$  to  $+10 \mu\text{A}$ .

tance  $d$  of the 2DEG from the sample surface is  $d = 37$  nm in our samples. The effective mass  $m^* = 0.07$  is deduced from the frequency of the cyclotron resonance, measured in the reference section. We fit our data by the  $(n_x, n_y) = (1, 0)$  mode and obtain very good agreement between theory and experiment. Therefore, the resonance in addition to the cyclotron resonance is identified as the fundamental  $(1, 0)$  or the degenerate  $(0, 1)$  magnetoplasmon mode in the superlattice.

Figure 3(a) shows photoconductivity spectra taken at a magnetic field of  $B = 8.0$  T (corresponding to a filling factor of  $\nu = 1.7$  of the 2DEG) for bias currents applied between source and drain contacts ranging from  $+10 \mu\text{A}$  to  $-10 \mu\text{A}$  in steps of  $2 \mu\text{A}$ . As expected, with no bias current applied no photoconductivity is observed (curve  $I = 0$ ). For bias currents of  $I = \pm 2 \mu\text{A}$  both the cyclotron resonance (CR) and the magnetoplasmon (MP) are observed in the photoresponse  $\Delta U_{xx}$  and have a large amplitude already. For higher bias currents up to  $I = \pm 10 \mu\text{A}$  the photoresponse amplitude in the cyclotron resonance slightly increases and finally decreases again. The photoresponse amplitude in the magnetoplasmon absorption, on the other hand, decreases monotonically.

Figure 3(b) shows data analogous to those in Fig. 3(a), but for a magnetic field of  $B = 6.8$  T, corresponding to a filling factor of  $\nu = 2$ . Under these conditions, up to high bias-currents of  $I = \pm 8 \mu\text{A}$ , only the cyclotron resonance is observed, but not the magnetoplasmon. Only for very high bias currents of  $I = \pm 10 \mu\text{A}$  does a magnetoplasmon-induced photoresponse begin to develop. The amplitude of the cyclotron resonance increases linearly with increasing bias current.

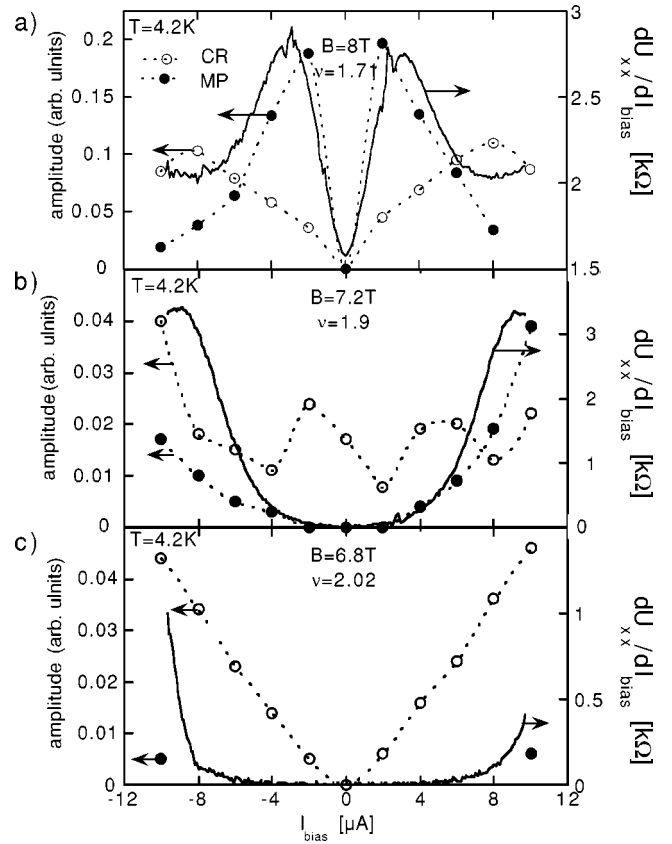


FIG. 4. Amplitudes of cyclotron resonance (open circles) and magnetoplasmon (solid dots) photoresponse in comparison to the longitudinal resistance  $dU_{xx}/dI_{bias}$  as a function of the bias current applied between source and drain.

For a filling factor of  $\nu = 1.9$  ( $B = 7.2$  T) (not shown) both the cyclotron resonance and the magnetoplasmon are observed in the photoresponse, but the magnetoplasmon only for bias currents higher than about  $I = \pm 3 \mu\text{A}$ .

Summarizing, at integer filling factor  $\nu = 2$  of the 2DEG only the cyclotron resonance is observed in photoresponse. At  $\nu < 2$  both the magnetoplasmon and the cyclotron resonance are observed in photoresponse.

Figure 4 shows the amplitudes of the spectra from Figs. 3(a) and 3(b) as a function of the bias current between source and drain. Open circles correspond to the cyclotron resonance maximum, black dots to the magnetoplasmon signal. The dashed interpolating lines are guides to the eye only. For comparison, the differential longitudinal resistance  $dU_{xx}/dI_{bias}$  as a function of the bias current, recorded in the same geometry as the photoresponse, is plotted (solid line).

#### IV. DISCUSSION

Figure 4 demonstrates that the amplitude of the magnetoplasmon signal qualitatively follows the differential longitudinal resistance  $dU_{xx}/dI_{bias}$  for different magnetic fields (filling factors). It will be shown in the following that therefore the magnetoplasmon signal can be explained by heating of the electron gas corresponding to the bolometric model.<sup>11</sup>

In the bolometric model the photoresponse of a sample is

regarded as a change in the voltage (or resistance, or conductivity, depending on whether a voltage, resistance or conductivity is measured in the specific sample geometry) caused by an increased electron temperature. In our case, the longitudinal voltage is measured in a four-point geometry (Fig. 1). Thus the photoresponse corresponds, in terms of the bolometric model, to a temperature-induced change in the longitudinal voltage  $\Delta U_{xx} = dU_{xx}/dT \Delta T$ . The increase in electron temperature,  $\Delta T$ , is provided by the resonant absorption of the THz radiation. Since the absorption coefficient does not strongly depend on magnetic field or filling-factor and since filling factor-induced oscillations of the electronic specific heat are rather weak, we can for simplicity assume that  $\Delta T$  does not depend on magnetic field or filling factor in the present, small signal limit. Thus, the photoresponse is determined by the dependence  $dU_{xx}/dT$  of the voltage  $U$  on temperature.

On the other hand, a sufficiently high bias current  $I$  also produces an increase in electron temperature. Thus the differential  $dU_{xx}/dI$  is directly proportional to  $dU_{xx}/dT$ .

The amplitude of the magnetoplasmon-induced photoresponse as a function of bias current  $I$  very closely resembles the differential longitudinal resistance  $dU_{xx}/dI$  and thus  $dU_{xx}/dT$ . Thus the bolometric model can describe the photoresponse mechanism at the magnetoplasmon resonance as heating of the electron gas.

A nonzero longitudinal voltage  $U_{xx}(T)$  is, on the other hand, a rough measure for the amount of conduction through bulk, dissipative electronic states.<sup>21</sup> Thus the appearance of the magnetoplasmon in photoconductivity can be taken as an indicator of beginning bulk conductivity.

For  $\nu = 1.7$  ( $B = 8$  T) the amplitude of the cyclotron resonance has a behavior similar to that of the magnetoplasmon [Fig. 4(a)], even though the features occur at higher bias currents. For  $\nu = 2$  or  $B = 6.8$  T [Fig. 4(c)], in contrast, the amplitude of the cyclotron resonance signal increases linearly with increasing bias current while the amplitude of the magnetoplasmon response and the longitudinal resistance (solid line) stay almost zero up to bias currents of  $I = \pm 8 \mu\text{A}$ . The suppression of the magnetoplasmon and the vanishing longitudinal resistance indicate that the 2D bulk is still insulating. Thus only the edge states contribute to the conductance at an external magnetic field of  $B = 6.8$  T ( $\nu = 2$ ). Therefore, we attribute the cyclotron resonance part of the photoresponse at  $\nu = 2$  to backscattering of the topmost edge states. At  $B = 8$  T probably both mechanisms are important, as will be discussed below.

Summarizing the discussion, the magnetoplasmon absorption leads to a photoresponse only in the dissipative transport regime, when the 2D bulk is conducting, which also manifests itself in a nonzero (differential) longitudinal magnetoresistance  $\rho_{xx} = dU_{xx}/dI$ . The cyclotron resonance absorption leads to a photoresponse also in the adiabatic transport regime, when only the edge states contribute to electric conductance.

As for the mechanism of backscattering we follow the argumentation of Diessel *et al.* and propose that the absorption of THz radiation at the cyclotron resonance in the regime of the QHE at  $\nu \approx 2$  leads to a nonequilibrium popula-

tion of edge states and thus to an enhanced interedge scattering rate, i.e., the rate of backscattering from one edge of the Hall bar through the insulating bulk region to the other edge.

In the case of an antidot superlattice as studied here, not only do extended edge states at the boundaries of the Hall bar exist, but also localized states around the antidots. We propose that backscattering in our superlattice takes place in several steps via the current loops localized around the antidots.

We will now briefly discuss our data for other different filling factors (magnetic fields). At a filling factor of  $\nu = 1.9$  ( $B = 7.2$  T) [Fig. 4(b)] the cyclotron resonance behaves as for  $\nu = 2$  ( $B = 6.8$  T) [Fig. 4(c)]. The magnetoplasmon amplitude and  $\rho_{xx}$  are both almost zero for small bias currents below  $2 \mu\text{A}$  and then increase very similarly to each other. This is explained as follows: For low bias currents below  $2 \mu\text{A}$  the sample is in an adiabatic state of conductance and only the cyclotron resonance absorption produces a photoresponse. For higher bias currents bulk transport is beginning to be thermally activated, such that the sample is now in a dissipative state. Correspondingly the magnetoplasmon absorption also generates a photoresponse.<sup>22</sup> At a magnetic field of  $B = 6.2$  T, still in the plateau region of  $\rho_{xx}$  around integer filling factor  $\nu = 2$  (not shown), the data are very similar to those for  $\nu = 2$  ( $B = 6.8$  T) [Fig. 4(c)]. The reason for this is, that—up to bias currents of  $10 \mu\text{A}$ —the 2DEG is still in an adiabatic state ( $\rho_{xx}$  is still vanishing). Thus only the CR absorption generates a photoresponse. For a filling factor of  $\nu = 1.6$  ( $B = 8.6$  T) (not shown), where  $\rho_{xx}$  is nonzero the data resemble those for  $\nu = 1.7$  ( $B = 8$  T) (where  $\rho_{xx} \neq 0$  as well) [Fig. 4(a)]. This is because the 2DEG is in a dissipative state. Thus both CR and MP absorption lead to a photoresponse.

Now it remains to be discussed *why* the magnetoplasmon is visible in the photoresponse in the dissipative transport regime only, but the cyclotron resonance occurs both in the dissipative and the adiabatic transport regimes, i.e., why only CR absorption is able to induce backscattering of edge states.

The extent of the edge states into the 2D bulk is comparable to the edge depletion length, which is of the order of a few 100 nm. The characteristic coherence length  $l$  of a collective excitation with a frequency/wave vector dependence  $\omega(q)$  is generally equal to  $l = (d\omega/dq)\tau$  with the scattering time  $\tau$ . For the magnetoplasmon in our samples this relation gives  $l \approx 10 \mu\text{m}$ . This means that the magnetoplasmon excitation has its full strength only a distance  $l \approx 10 \mu\text{m}$  away from the sample boundaries, i.e., deep in the 2D bulk. At the location of the edge states, not much more than 100 nm away from the boundaries, the magnetoplasmon has almost vanished. When only the edge states contribute to electric conduction, as is the case under adiabatic transport conditions, the magnetoplasmon in the 2D bulk cannot be converted into a photoresponse. This conversion could only be done by the edge states, but at the location of the edge states the magnetoplasmon oscillation strength is already negligible.

The characteristic length for the cyclotron resonance is the magnetic length. Even though the cyclotron resonance as a collective phenomenon is affected by finite-size effects up

to macroscopic dimensions,<sup>23</sup> it is sensitive to the local potential landscape even in the nanometer range.<sup>24</sup> Thus absorption in the cyclotron resonance can be converted into a photoresponse by the edge states also.

## V. CONCLUSION

We have examined cyclotron-resonance- and magnetoplasmon-induced changes in the longitudinal voltage of an antidot superlattice in high magnetic fields by means of photoconductivity measurements. In the dissipative transport regime we detect both magnetoplasmon and cyclotron resonances in the photoresponse. In the adiabatic transport regime at integer bulk filling factor  $\nu=2$  we detect only the cyclotron resonance in the photoresponse. To explain these experimental results, i.e., the different dependencies of the amplitudes of the photoresponse in the cyclotron resonance and in the magnetoplasmon resonance on the applied bias current at different filling factors, we suggest a model wherein different mechanisms generate photoconductivity in the magnetoplasmon resonance and in the cyclotron reso-

nance. According to this model electron heating is responsible for photoconductivity in the dissipative transport regime. In the regime of adiabatic transport at integer filling factor  $\nu=2$  the photoresponse is generated by backscattering of the topmost edge state, and this backscattering can be caused by the cyclotron resonance only.

The reason that only the CR can cause backscattering of edge states is that cyclotron and magnetoplasmon resonances have different characteristic lengths. The characteristic length of the cyclotron resonance is comparable to the lateral extent of the edge states; thus CR absorption can induce backscattering of edge states. The characteristic length of the magnetoplasmon is larger by almost an order of magnitude than the lateral extent of the edge states; thus MP absorption *cannot* induce backscattering of edge states.

## ACKNOWLEDGMENTS

We would like to acknowledge Alik Chaplik and Achim Wixforth for valuable discussions and the Deutsche Forschungsgemeinschaft for financial support.

\*Present address: Institut für Angewandte Physik, Universität Regensburg, 93040 Regensburg, Germany.

<sup>1</sup>M. Büttiker, Phys. Rev. B **38**, 6375 (1988).

<sup>2</sup>R. Landauer, IBM J. Res. Dev. **1**, 223 (1957).

<sup>3</sup>P. Streda, J. Kucera, and A. H. MacDonald, Phys. Rev. Lett. **59**, 1973 (1987).

<sup>4</sup>J. K. Jain and S. A. Kivelson, Phys. Rev. Lett. **60**, 1542 (1988).

<sup>5</sup>R. B. Laughlin, Phys. Rev. B **23**, 5632 (1981).

<sup>6</sup>B. I. Halperin, Phys. Rev. B **25**, 2185 (1982).

<sup>7</sup>D. B. Chklovskii, B. I. Shklovskii, and L. I. Glazman, Phys. Rev. B **46**, 4026 (1992).

<sup>8</sup>P. L. McEuen, A. Szafer, C. A. Richter, B. W. Alphenaar, J. K. Jain, A. D. Stone, R. G. Wheeler, and R. N. Sacks, Phys. Rev. Lett. **64**, 2062 (1990).

<sup>9</sup>S. Komiyama, H. Hirai, M. Ohsawa, Y. Matsuda, S. Sasa, and T. Fujii, Phys. Rev. B **45**, 11 085 (1992).

<sup>10</sup>Y. Shiraki, J. Phys. C **10**, 4539 (1977).

<sup>11</sup>F. Neppel, J. P. Kotthaus, and J. F. Koch, Phys. Rev. B **19**, 5240 (1979).

<sup>12</sup>A. Darr, A. Huber, and J. P. Kotthaus, *Proceedings of the 3rd International Conference on the Physics of Narrow Gap Semiconductors*, edited by J. Rauluszkiwicz (PWN Polish Scientific, Warsaw, 1978), p. 418; J. C. Maan, Th. Englert, D. C. Tsui, and A. C. Gossard, Appl. Phys. Lett. **40**, 609 (1982); F. Thiele, E. Batke, V. Dolgoplov, J. P. Kotthaus, G. Weimann, and W. Schlapp, Phys. Rev. B **40**, 1414 (1989); A. Lorke, J. P. Kotthaus, J. H. English, and A. C. Gossard, *ibid.* **53**, 1054 (1996); K. Hirakawa *et al.*, in *Proceedings of the 23rd International Conference on the Physics of Semiconductors*, edited by M. Scheffler *et al.* (World Scientific, Singapore, 1996), p. 2543.

<sup>13</sup>H. Drexler, W. Hansen, J. P. Kotthaus, M. Holland, and S. P. Beaumont, Appl. Phys. Lett. **64**, 2270 (1994); E. Vasiliadou *et al.*, Phys. Rev. B **52**, R8658 (1995); C. M. Engelhardt, R.

Strenz, M. Aschauer, G. Böhm, G. Weimann, V. Rosskopf, and E. Gornik, in *Proceedings of the 11th International Conference on High Magnetic Fields in Semiconductor Physics, Cambridge, MA*, edited by D. Heiman (World Scientific, Singapore, 1994), p. 504.

<sup>14</sup>R. Merz, F. Keilmann, R. J. Haug, and K. Ploog, Phys. Rev. Lett. **70**, 651 (1993).

<sup>15</sup>E. Diessel, G. Müller, D. Weiss, K. von Klitzing, K. Ploog, H. Nickel, W. Schlapp, and R. Lösch, Europhys. Lett. **24**, 785 (1993); Appl. Phys. Lett. **58**, 2231 (1991).

<sup>16</sup>A. Lorke, S. Wimmer, B. Jäger, J. P. Kotthaus, W. Wegscheider, and M. Bichler, Physica B **249**, 312 (1998); B. G. L. Jäger *et al.* (unpublished).

<sup>17</sup>A. V. Chaplik, Surf. Sci. Rep. **5**, 289 (1985); A. V. Chaplik, Zh. Éksp. Teor. Fiz. **62**, 746 (1972) [ Sov. Phys. JETP **35**, 395 (1972)].

<sup>18</sup>F. Stern, Phys. Rev. Lett. **18**, 546 (1967).

<sup>19</sup>G. Eliasson, P. Hawrylak, and J. J. Quinn, Phys. Rev. B **36**, 7631 (1986).

<sup>20</sup>T. N. Theis, J. P. Kotthaus, and P. J. Stiles, Solid State Commun. **24**, 273 (1977).

<sup>21</sup>K. von Klitzing, Physica B & C **126B**, 242 (1984); *The Quantum Hall Effect*, edited by R. E. Prange and M. Girvin (Springer, New York, 1987).

<sup>22</sup>This change of state from adiabatic to dissipative, taking place around  $2 \mu\text{A}$ , could also explain the peculiar nonmonotonic behavior of the CR signal at  $\nu=1.9$ . The strength of the signal caused by edge state backscattering is likely to be reduced when dissipative transport sets in, so that the total signal drops before increasing again at higher biases.

<sup>23</sup>E. Vasiliadou *et al.*, Phys. Rev. B **48**, 17 145 (1993).

<sup>24</sup>See, e.g., U. Merkt, Phys. Rev. Lett. **76**, 1134 (1996), and references therein.